



Computerized evaluation scheme to detect metastasis in sentinel lymph nodes using contrast-enhanced computed tomography before breast cancer surgery

Hiroshi Ashiba^{1,2} · Ryohei Nakayama³

Received: 15 July 2018 / Revised: 19 November 2018 / Accepted: 21 November 2018 / Published online: 29 November 2018
© Japanese Society of Radiological Technology and Japan Society of Medical Physics 2018

Abstract

Sentinel lymph node (SLN) biopsy for evaluating lymph node metastasis during breast cancer surgery is associated with several problems, such as the consequent increase in operation time and the possibility of abrupt changes in the treatment plan during the operation. Although it is desirable to distinguish SLNs with and without cancer metastasis before surgery, there is no established examination for this purpose. This study aimed to develop a computerized scheme for evaluating metastasis in SLNs by analyzing computed tomography lymphography images and the three-dimensional versions of these images. Our database consisted of computed tomography lymphography images from 100 patients with breast cancer. Three subjective features of the nodes were assessed in the three-dimensional images: (1) the shape of the lymphoduct, (2) degree of signal enhancement in the nodes, and (3) shape of the nodes. Six objective features were also assessed in the computed tomography lymphography images: (4) the long axis, (5) area, (6) standard deviation of the signal values, (7) mean signal values, (8) maximum signal value, and (9) minimum signal value. Support vector machines were employed to evaluate cancer metastasis in SLNs. For the input, six of the nine features were selected in a stepwise method. The classification accuracy, sensitivity, and specificity were 98.0% (98/100), 97.8% (44/45), and 98.2% (54/55), respectively. The positive and negative predictive values were 97.8% (44/45) and 98.2% (54/55), respectively. This computerized method exhibited high classification accuracy and will be useful in determining the need for lymph node dissection before breast cancer surgery.

Keywords Sentinel lymph node · CT lymphography · Breast cancer · Metastasis

1 Introduction

Recent reports have suggested that approximately 1 in 20 women are affected by breast cancer in Japan. The incidence of breast cancer is the highest among cancers in

female patients [1]. Approximately 40,000 de novo cases of breast cancer are reported annually, and approximately 10,000 breast cancer patients die each year [2]. The number of cases requiring breast cancer surgery has also been increasing annually with the incidence of breast cancer [3]. In breast cancer surgery, axillary lymph node dissection, which removes all lymph nodes surrounding the breast, is recommended when the cancer has spread to the lymph nodes. However, this often causes complications such as contracture of the shoulder joint, upper limb edema, and paralysis. These complications decrease the patient's quality of life. In clinical practice, cancer metastasis in the lymph nodes is diagnosed by biopsy of the sentinel lymph node (SLN) during breast cancer surgery. The SLN is the first lymph node to receive lymph flow from the tumor [4, 5]. The decision to perform axillary lymph node dissection is based on the biopsy result. However, SLN biopsy is associated with several problems, such as the consequent increase in operation time and the possibility of abrupt changes in the

✉ Hiroshi Ashiba
ashibe1@yahoo.co.jp

Ryohei Nakayama
ryohei@fc.ritsumeikan.ac.jp

¹ Department of Radiology, Maruyama Memorial General Hospital, 2-10-5 Hon-cho, Iwatsuki-ku, Saitama 339-8521, Japan

² Graduate School of Health Science, Suzuka University of Medical Science, 1000-1 Kishioka-cho, Suzuka 510-0293, Japan

³ Department of Electronic and Computer Engineering, Ritsumeikan University, 1-1-1 Noji-higashi, Kusatsu, Shiga 525-8577, Japan

treatment plan during the operation. Although it is desirable to distinguish SLNs with and without cancer metastasis before surgery, there is no established examination for this purpose.

Yamamoto et al. reported that the lymphoducts and SLNs in 549 of 576 patients with breast cancer (96%) could be identified in computed tomography lymphography (CTLG) images with lymphangiography [6]. After SLNs were identified in CTLG images, 81% of the SLNs with a cortical thickness of ≥ 2.5 cm in ultrasonography were identified as cases of cancer metastasis in their study [7]. Suga et al. concluded that the features of early breast cancer are visible in CTLG images [8]. Nakagawa et al. defined imaging features such as dilated/stagnating/tortuous lymphoducts and SLNs with heterogeneous contrast as findings indicating metastasis in three-dimensional (3D) images generated from CTLG images using workstations [9]. They distinguished 228 SLNs with and without metastasis on the basis of these findings. The classification accuracy, sensitivity, and specificity were 89.0%, 92.6%, and 88.6%, respectively. The positive predictive value was 52.1%, whereas the negative predictive value was 98.8%. We considered that, in addition to the features in 3D CTLG images, other features such as the computed tomography (CT) value and the area of the SLN in CTLG images may be useful for metastasis evaluation. In this study, we developed a computerized scheme for evaluating metastasis in SLN by analyzing CTLG images and their 3D versions.

2 Materials and methods

The use of the following database was approved by the Institutional Review Board of Maruyama Memorial General Hospital (the approval number: 2008-1).

2.1 Materials

Our database consisted of CTLG images from 100 patients with breast cancer who underwent surgery at Maruyama Memorial General Hospital from December 2009 to October 2014. The number of patients with SLN metastasis was 45, whereas that without SLN metastasis was 55. Table 1 provides the patients' clinical information (age, histological classification, and grade of the primary tumors). All CT images were obtained with a 64-detector row CT scanner (Perspective64; Siemens Healthcare, Erlangen, Germany). The imaging parameters were a detector configuration of 64×0.6 mm collimation, tube voltage of 130 kVp, quality ref of 100 mAs, auto exposure control (CARE Dose 4D), gantry rotation time of 0.6 s, pitch factor of 1.15, matrix size of 512×512 , and field of view of 300 mm. The 3D reconstruction parameters were a slice spacing of 1 mm and slice thickness of 1 mm. The CTLG images were mean 2D axial slice images, and the 3D CTLG images were generated from the CTLG images using a workstation (Aquarius WS, TeraRecon, Inc., Foster City, CA, USA). All SLNs of the tumors in our database underwent biopsy. The SLNs in the CTLG images and their 3D versions were identified by two experienced breast surgeons. The CTLG scan and biopsy were performed using the following procedures [10–12].

Before breast cancer surgery:

1. Injection of 3 cc contrast agent (iopamidol 300) for CT into the skin of the areola
2. Scanning CT with a slice thickness of 1 mm after massage for 3 min
3. Identification of the lymph node that first received the contrast agent as the SLN of the tumor observed in the CTLG images
4. Marking the estimated location of the SLN on the body surface on the basis of the CTLG images

Table 1 Patients' clinical information (age, histological classification, and grade of the primary tumors)

	With SLN metastasis	Without SLN metastasis	Histological classification	With SLN metastasis	Without SLN metastasis
Age					
<40	4	4	Noninvasive ductal carcinoma	1	6
41–50	13	9	Lobular carcinoma in situ	1	1
51–60	12	12	Papillotubular carcinoma	5	8
61–70	11	23	Solid-tubular carcinoma	19	14
71>	5	7	Scirrhous carcinoma	13	20
Grade			Mucinous carcinoma	3	3
1	19	42	Medullary carcinoma	1	0
2	13	6	Invasive lobular carcinoma	1	2
3	13	7	Apocrine carcinoma	1	1

During breast cancer surgery:

1. Identification of the SLN using the dye method [13, 14], with injection of 5 cc indigo carmine into the skin of the areola
2. Implementation of biopsy for the identified SLN

2.2 Feature extraction

Three radiological technologists who were engaged in breast cancer treatment independently evaluated the following subjective features for each SLN in the 3D CTLG images: (1) the shape of the lymphoduct (discontinuous/tapering/normal), (2) degree of enhancement in the SLN (none/heterogeneous/complete), and (3) shape of the SLN (irregular/oval/round). Here, the lymphoduct and SLN were segmented automatically by analyzing the contrast agent concentration in the CTLG images using the workstation [6]. Fig. 1 provides an example of the segmented SLNs and lymphoducts. Finally, the subjective features for each SLN were determined by consensus among the three radiological technologists. In addition, six objective features in the CTLG images were determined using a DICOM viewer. The objective features of the SLNs were as follows: (4) the long axis, (5) area, (6) standard deviation of the CT values, (7) mean CT value, (8) maximum CT value, and (9) minimum CT value.

2.3 Classification scheme

In this study, a support vector machine (SVM) [15, 16], which is a classifier, was employed to evaluate cancer metastasis in SLNs. The SVM provides, theoretically, a separating hyperplane with the largest margin between two classes, and

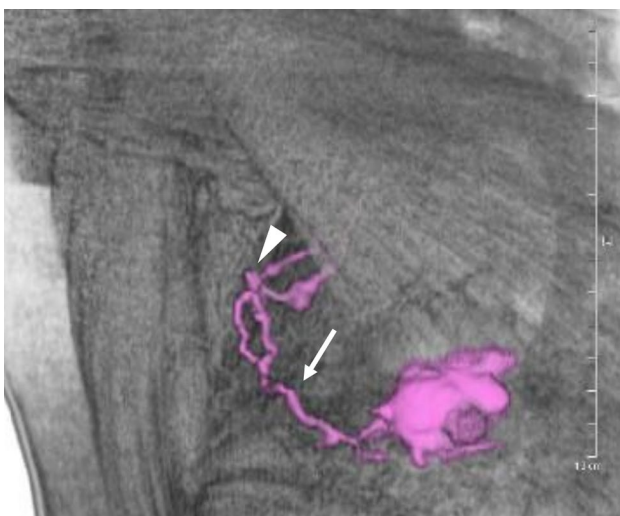


Fig. 1 Example of a sentinel lymph node (arrowhead) and a lymphoduct (arrow) segmented using a workstation

also a nonlinear discrimination function for the separating hyperplane with kernel transformation [17]. With these properties, the SVM is expected to achieve better recognition performance than that achieved by conventional classifiers. In this study, a SVM with a nonlinear radial basis function was employed to evaluate cancer metastasis in SLNs. The hyper-parameters of the SVM were determined with a Bayesian optimization [18].

The features used as inputs for the SVM were selected from the nine aforementioned features according to a stepwise method based on Wilks's lambda [19]. The stepwise method first selected the feature with the lowest Wilks's lambda for entry into the SVM. Next, another feature was selected such that the overall Wilks's lambda was minimized for the combination of the selected features. This procedure was repeated until the overall Wilks's lambda did not decrease further. A leave-one-out testing method [20] was used for the training and testing of the SVM. In this method, the training was performed for all but one of the cases in the database; the case not used for training was used for testing with the trained SVM. This procedure was repeated until every case in our database had been used once.

3 Results

The agreement rates of subjective features by the three observers were 94% for the shape of the lymphoduct, 95% for the degree of enhancement, and 96% for the shape of the SLN. Table 2 presents the results of tests for univariate equality of group means for each of the nine features. The Wilks's lambda for the degree of enhancement in the SLN was the smallest of the nine features, indicating that this feature exhibited the largest discrepancy between SLNs with and without metastasis. Although the maximum CT value of the SLN had the largest Wilks's lambda, it satisfied the significance level (i.e., $P < .001$).

Table 2 Results of tests for univariate equality of group means for each of the nine features

Features	Wilk's lambda	P value
Shape of lymphoduct	0.462	< .001
Degree of signal enhancement for SLN	0.313	< .001
Shape of SLN	0.527	< .001
Long axis of SLN	0.492	< .001
Area of SLN	0.597	< .001
Standard deviation of CT values of SLN	0.832	< .001
Mean CT value of SLN	0.737	< .001
Maximum CT value of SLN	0.868	< .001
Minimum CT value of SLN	0.863	< .001

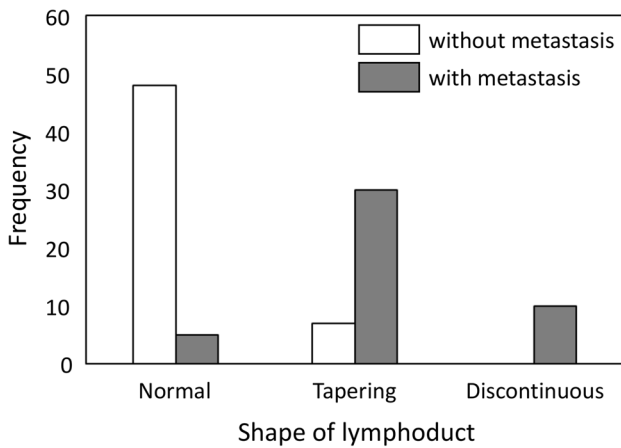


Fig. 2 Histogram of the shape of a lymphoduct

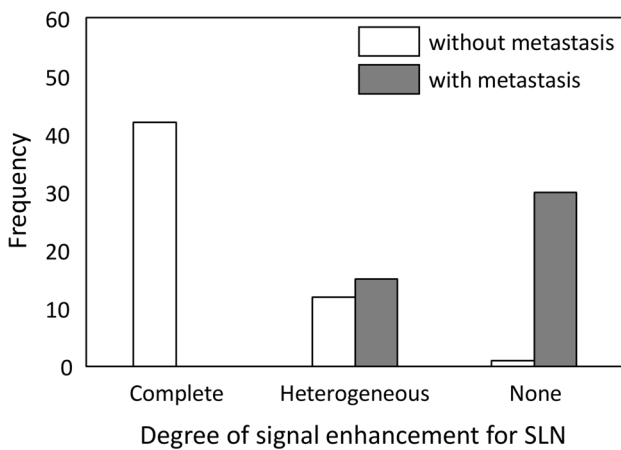


Fig. 3 Histogram of the degree of signal enhancement for a sentinel lymph node. *SLN* sentinel lymph node

The six features used for the SVM were selected from the nine features using the stepwise method, based on the Wilks's lambda. These features were as follows: (1) the shape of the lymphoduct, (2) degree of enhancement of the SLN, (3) long axis of the SLN, (4) area of the SLN, (5) standard deviation of CT values of the SLN, and (6) mean CT value of the SLN. Figure 2 presents the histogram of the shapes of the lymphoduct, while Fig. 3 presents the histogram of the degrees of enhancement of the SLN signal. The SLNs with metastasis tended to have a disconnected and vanishing lymphoduct, and also tended to be difficult to contrast. Figure 4 illustrates the relationship between the long axis and the area of the SLNs, and Fig. 5 illustrates the relationship between the standard deviation and the mean CT value of the SLNs. Both the long axes and the areas of the SLNs with metastasis tended to be larger than that of those without metastasis, whereas the standard deviation and mean CT value of the SLNs with

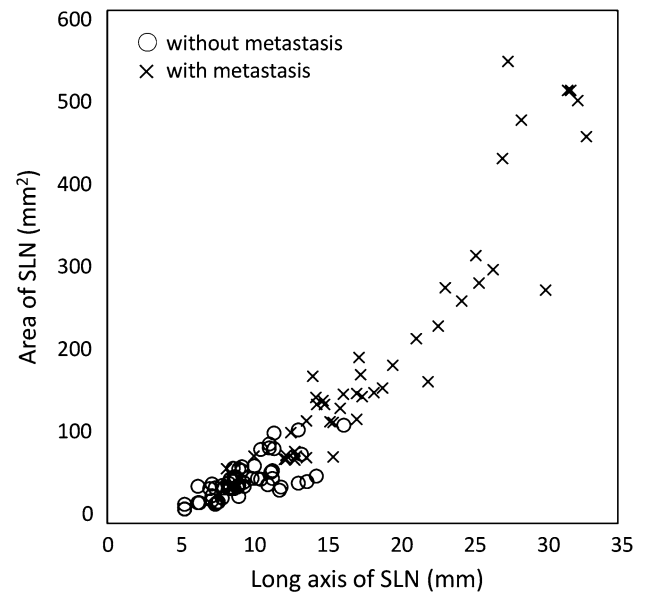


Fig. 4 Relationship between the long axis and area of sentinel lymph nodes. *SLN* sentinel lymph node

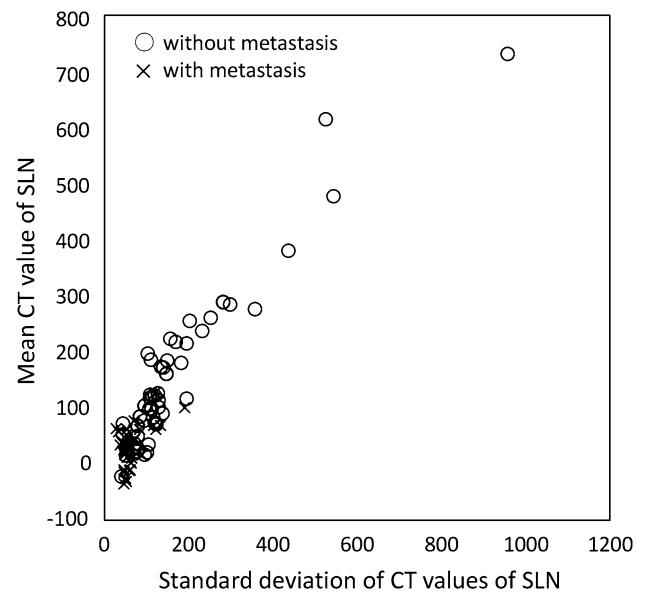


Fig. 5 Relationship between the standard deviation and mean computed tomography value of sentinel lymph nodes. *CT* computed tomography, *SLN* sentinel lymph node

metastasis appeared to be lower than that of those without metastasis.

Table 3 provides the computerized classification results with the SVM using the six features selected by the stepwise method. The classification accuracy, sensitivity, and specificity were 98.0% (98/100), 97.8% (44/45), and 98.2% (54/55), respectively. The positive and negative predictive values were 97.8% (44/45) and 98.2% (54/55), respectively.

Table 3 Computerized classification results obtained with the support vector machine using the six features selected by the stepwise method

	Computer output	
	With metastasis	Without metastasis
With metastasis (45)	97.8% (44/45)	2.2% (1/45)
Without metastasis (55)	1.8% (1/55)	98.2% (54/55)

In the receiver operating characteristic (ROC) analysis [21], the area under the ROC curve (AUC) was 0.972.

4 Discussion

To evaluate the utility of combining the features determined from the 3D CTLG images and the CTLG images in distinguishing SLNs with and without metastasis, we employed SVMs with only the features from the 3D CTLG and those with only the features from CTLG. Using the stepwise method, all three subjective features (i.e., features i–iii) were selected for the SVM for 3D CTLG. Five objective features (i.e., features iv–viii), excluding the minimum CT value, were selected for the SVM for CTLG. The classification accuracy, sensitivity, specificity, positive predictive value, and negative predictive value for the SVM for 3D CTLG were 93.0% (93/100), 91.1% (41/45), 94.5% (52/55), 93.2% (41/44), and 92.9% (52/56), respectively, whereas those for the SVM for CTLG were 95.0% (95/100), 93.3% (42/45), 96.4% (53/55), 95.5% (42/44), and 94.6% (53/56), respectively. The results for CTLG were greater than those for 3D CTLG. The AUC for the SVM with both 3D CTLG and CTLG was significantly greater than those for the SVMs with 3D CTLG (AUC = 0.923, $P = .013$) and with CTLG (AUC = 0.947, $P = .038$). These results improved substantially by combining the features from 3D CTLG and CTLG, implying that such a combination could significantly contribute to the distinction of SLNs with and without metastasis.

In clinical practice, it is important to assess the CT values in CT examination. Therefore, we also employed the SVM with the five features (i.e., features i–v), excluding the features of CT values, to distinguish SLNs with and without metastasis. Using the stepwise method, four features (i.e., features i–iv), excluding the area of the SLN, were selected as the inputs of the SVM. The classification accuracy, sensitivity, specificity, positive predictive value, and negative predictive value for the SVM excluding the features of CT values were 93.0% (93/100), 88.9% (40/45), 96.4% (53/55), 95.2% (40/42), and 91.4% (53/58), respectively. The AUC was also 0.915 ($P = .010$). Relatively low classification accuracy was obtained when the features of CT values were excluded from the SVM. This result

implies that the contribution of the features of CT values to the distinction of SLNs with and without metastasis was not small.

As a further step in evaluating the utility of the stepwise method, we employed the SVM with all the nine features that were determined in this study. The classification accuracy, sensitivity, and specificity were 95.0% (95/100), 93.3% (42/45), and 96.4% (53/55), respectively. The positive and negative predictive values were 95.5% (42/44) and 94.6% (53/56), respectively. All values were lower than those obtained with the SVM based on the six features selected from the nine features according to the stepwise method. The AUC for the SVM with all the nine features (AUC = 0.952, $P = .044$) was significantly lower than that for the SVM based on the stepwise method. This implies that the stepwise method was indeed useful in selecting the features as inputs for the SVM.

There have been a few previous studies on the prediction of SLN metastasis from magnetic resonance (MR) images [22, 23]. These studies used a large number of quantitative features, and achieved relatively high classification performance. MR imaging (MRI) involves no radiation exposure but the imaging time is long. Both CT and MRI contribute advantages and disadvantages in clinical practice. Therefore, it is difficult to evaluate which of CT and MRI is more useful in predicting SLN metastasis. However, we believe that CT might provide more essential features for predicting SLN metastasis than MRI because a small number of features extracted from CT images achieved a sufficiently high classification accuracy in this study.

With the proposed method, the classification accuracy, sensitivity, and specificity were 98.0%, 97.8%, and 98.2%, respectively. The proposed method achieved high classification performance for distinguishing SLNs with and without metastasis before breast cancer surgery. This method must be further validated using a larger database to demonstrate the feasibility of employing it instead of SLN biopsy in clinical practice. However, the proposed method is likely to prevent an abrupt change in the planning of the surgical procedure due to necessary/unnecessary lymph node dissection.

There are some limitations to this study. First, the lymph nodes and SLNs were segmented automatically using a workstation to determine the features from 3D CTLG. There may be some variations among the different types of workstations in the segmented regions generated. Thus, the segmented regions generated using different types of workstations should be cross-checked for replicability. Second, the features from 3D CTLG were evaluated subjectively by three experienced radiological technologists. We believe that bias was minimal because the results of the SLN biopsies were not provided to them. However, objective quantitative methods for these features are desirable for further studies.

5 Conclusion

We developed a computerized scheme for distinguishing SLNs with and without metastasis using a combination of the features from 3D CTLG and CTLG images. The proposed method exhibited high classification accuracy and may be useful in determining whether to implement lymph node dissection before breast cancer surgery.

Acknowledgements The authors are grateful to the members of the Department of Radiology, Maruyama Memorial General Hospital, for supporting this work.

Compliance with ethical standards

Conflict of interest The authors declare that they have no conflict of interest.

Ethical approval For this type of study, formal consent is not required at our Institution. This article does not contain any studies with animals performed.

Informed consent Informed consent was obtained from all individual participants included in the study.

References

- Hori M, Matsuda T, Shibata A, Katanoda K, Sobue T, Nishimoto H. Cancer incidence and incidence rates in Japan in 2009: a study of 32 population-based cancer registries for the Monitoring of Cancer Incidence in Japan (MCIJ) project. *Jpn J Clin Oncol*. 2015;45:884–91.
- National Cancer Center. Cancer Registry and Statistics Japan. *Cancer Inf Serv*. 2014;105:1480–6.
- Kurebayashi J, Miyoshi Y, Ishikawa T, Saji S, Sugie T, Suzuki T, Takahashi S, Nozaki M, Yamashita H, Tokuda Y, Nakamura S. Clinicopathological characteristics of breast cancer and trends in the management of breast cancer patients in Japan: based on the Breast Cancer Registry of the Japanese Breast Cancer Society between 2004 and 2011. *Breast Cancer*. 2015;22:235–44.
- Schwartz GF, Giuliano AE, Veronesi U. Proceedings of the consensus conference on the role of sentinel lymph node biopsy in carcinoma of the breast April 19 to 22, 2001, Philadelphia, Pennsylvania. *Cancer*. 2002;94:2542–51.
- Kuehn T, Bembenek A, Decker T. A concept for the clinical implementation of sentinel lymph node biopsy in patients with breast carcinoma with special regard to quality assurance. *Cancer*. 2005;103:451–61.
- Yamamoto S, Suga K, Maeda K, Maeda N, Yoshimura K, Oka M. Breast sentinel lymph node navigation with three-dimensional computed tomography–lymphography: a 12-year study. *Breast Cancer*. 2016;23:456–62.
- Yamamoto S, Maeda N, Tamesa M, Nagashima Y, Yoshimura K, Oka M. Prospective ultrasonographic prediction of sentinel lymph node metastasis by real-time virtual sonography constructed with three-dimensional computed tomography–lymphography in breast cancer patients. *Breast Cancer*. 2012;19:77–82.
- Suga K, Yamamoto S, Tangoku A, Oka M, Kawakami Y, Matsunaga N. Breast sentinel lymph node navigation with three-dimensional interstitial multidetector-row computed tomographic lymphography. *Invest Radiol*. 2005;40:336–42.
- Nakagawa M, Morimoto M, Takechi H, Tadokoro Y, Tangoku A. Preoperative diagnosis of sentinel lymph node (SLN) metastasis using 3D CT lymphography (CTLG). *Breast Cancer*. 2016;23:519–24.
- Tangoku A, Yamamoto S, Suga K, Ueda K, Nagashima Y, Hida M, Sato T, Sakamoto K, Oka M. Sentinel lymph node biopsy using computed tomography–lymphography in patients with breast cancer. *Surgery*. 2004;135:258–65.
- Suga K, Ogasawara N, Yuan Y, Okada M, Matsunaga N, Tangoku A. Visualization of breast lymphatic pathways with an indirect computed tomography lymphography using a nonionic monometric contrast medium iopamidol: preliminary results. *Invest Radiol*. 2003;38:73–84.
- Minato M, Hirose C, Sasa M, Nishitani H, Hirose Y, Morimoto T. 3-dimensional computed tomography lymphography-guided identification of sentinel lymph nodes in breast cancer patients using subcutaneous injection of nonionic contrast medium: a clinical trial. *J Comput Assist Tomogr*. 2004;28:46–51.
- Giuliano AE, Kirgan DM, Guether V. Lymphatic mapping and sentinel lymphadenectomy for breast cancer. *Ann Surg*. 1994;220:391–8.
- Borgstein PJ, Meijer S, Pijpers R. Intradermal blue dye to identify sentinel lymph-node in breast cancer. *Lancet*. 1997;384:149–57.
- Vapnik V, Lerner A. Pattern recognition using generalized portrait method. *Automat Rem Contr*. 1963;24:774–80.
- Tsochantaridis I, Joachims T, Hofmann T, Altun Y. Large margin methods for structured and interdependent output variables. *J Mach Learn Res*. 2005;6:1453–84.
- Cortes C, Vapnik V. Support-vector networks. *Mach Learn*. 1995;20:273–97.
- Bergstra J, Bengio Y. Random search for hyper-parameter optimization. *J Mach Learn Res*. 2012;13:281–305.
- Chen W, Giger ML, Lan L, Bick U. Computerized interpretation of breast MRI: investigation of enhancement-variance dynamics. *Med Phys*. 2004;31:1076–82.
- Kuncheva LI. Combining pattern classifiers: methods and algorithms. New York: Wiley; 2004.
- Dorfman DD, Berbaum KS, Metz CE. Receiver operating characteristic rating analysis. Generalization to the population of readers and patients with the jackknife method. *Invest Radiol*. 1992;27:723–31.
- Liu C, Ding J, Spuhler K, Gao Y, Serrano Sosa M, Moriarty M, Hussain S, He X, Liang C, Huang C. Preoperative prediction of sentinel lymph node metastasis in breast cancer by radiomic signatures from dynamic contrast-enhanced MRI. *Magn Reson Imaging*. 2018 (**Epub ahead of print**).
- Dong Y, Feng Q, Yang W, Lu Z, Deng C, Zhang L, Lian Z, Liu J, Luo X, Pei S, Mo X, Huang W, Liang C, Zhang B, Zhang S. Preoperative prediction of sentinel lymph node metastasis in breast cancer based on radiomics of T2-weighted fat-suppression and diffusion-weighted MRI. *Eur Radiol*. 2018;28:582–91.